Ice-nucleating efficiency of aerosol particles and possible sources at three coastal marine sites

Meng Si[1], Victoria E. Irish[1], Ryan H. Mason[1], Jesús Vergara-Temprado[2], Sarah Hanna[1], Luis A. Ladino[3*], Jacqueline D. Yakobi-Hancock[3], Corinne L. Schiller[4], Jeremy J. B. Wentzell[5], Jonathan P. D. Abbatt[3], Ken S. Carslaw[2], Benjamin J. Murray[2], Allan K. Bertram[1]

[1]Department of Chemistry, University of British Columbia, Vancouver, V6T1Z1, Canada
[2]Institute for Climate and Atmospheric Science, School of Earth and Environment, University of Leeds, Leeds, LS2 9JT, UK
[3]Department of Chemistry, University of Toronto, Toronto, M5S3H6, Canada
[*]Now at: Centro de Ciencias de la Atmósfera, Universidad Nacional Autónoma de México, Ciudad Universitaria, Mexico City, Mexico
[4]Air Quality Science Unit, Environment and Climate Change Canada, Vancouver, V6C3S5, Canada
[5]Air Quality Research Division, Environment and Climate Change Canada, Toronto, M3H5T4, Canada

Correspondence to: Allan Bertram (bertram@chem.ubc.ca)

Abstract. Despite the importance of ice-nucleating particles (INPs) for climate and precipitation, our understanding of these particles is far from complete. Here, we investigated INPs at three coastal marine sites in Canada, two at mid-latitude (Amphitrite Point and Labrador Sea), and one in the Arctic (Lancaster Sound). At all three sites, the ice-nucleating efficiency on a per number basis (expressed as the fraction of aerosol particles acting as an INP) was strongly dependent on the size. For example, at diameters of around 0.2 µm, approximately 1 in 10^6 particles acted as an INP at -25 ºC, while at diameters of around 8 µm, approximately 1 in 10 particles acted as an INP at -25 ºC. The ice-nucleating efficiency on a per surface area basis (expressed as the surface active site density, n_s) was also dependent on the size, with larger particles being more efficient at nucleating ice. The n_s values of supermicron particles at Amphitrite Point and Labrador Sea were larger than previously measured n_s values of sea spray aerosol, suggesting that sea spray aerosol was not a major contributor to the supermicron INP population at these two sites. Consistent with this observation, a global model of INP concentrations under-predicted the INP concentrations when assuming only marine organics as INPs. On the other hand, assuming only K-feldspar as INPs, the same model was able to reproduce the measurements at a freezing temperature of -25 ºC, but under-predicted INP concentrations at -15 ºC, suggesting that the model is missing a source of INPs active at a freezing temperature of -15 ºC..

1 Introduction

Aerosol particles are ubiquitous in the atmosphere, yet only a small fraction of these particles are able to initiate the formation of ice at temperatures warmer than approximately -35 ºC (Hoose and Möhler, 2012). Aerosol particles that can initiate ice formation at temperatures above -35 ºC are referred to as ice-nucleating particles (INPs), and these particles can

significantly impact the frequencies, lifetime, and optical properties of ice and mixed-phase clouds (Andreae and Rosenfeld, 2008; Cziczo and Abbatt, 2001; Lohmann and Feichter, 2005).

It is now well established that mineral dust particles represent a large fraction of INPs in the atmosphere. For example, laboratory studies have shown that mineral dust particles are efficient at nucleating ice (Atkinson et al., 2013; Boose et al.,

5   2016a; Broadley et al., 2012; Eastwood et al., 2008; Field et al., 2006; Hartmann et al., 2016; Hiranuma et al., 2015; Hoose and Möhler, 2012; Kanji and Abbatt, 2010; Knopf and Koop, 2006; Murray et al., 2011; Wex et al., 2014). Field measurements have shown that mineral dust is a main component of INPs at different locations (Boose et al., 2016b; DeMott et al., 2003; Klein et al., 2010; Prenni et al., 2009; Worringen et al., 2015). Modeling studies have also suggested that mineral dust particles are a major contributor to INP concentrations in many locations around the globe (Hoose et al., 2010;

10   Vergara-Temprado et al., 2017).

Recent studies also suggest that sea spray aerosol may be an important source of INPs in some remote marine regions. For example, field and laboratory measurements have shown that the sea-surface microlayer and bulk seawater can contain INPs (Alpert et al., 2011a, 2011b; Burrows et al., 2013; DeMott et al., 2016; Irish et al., 2017; Knopf et al., 2011; Rosinski et al., 1986, 1988; Schnell, 1977; Schnell and Vali, 1976, 1975; Wang et al., 2015; Wilson et al., 2015), and these INPs are thought

15   to be emitted into the atmosphere by the bubble bursting mechanism (DeMott et al., 2016; Wang et al., 2015). Field measurements and modeling studies also suggest that sea spray aerosol is a major source of INPs in some remote marine environments removed from other sources of INPs (Burrows et al., 2013; Rosinski et al., 1988; Schnell, 1982; Vergara-Temprado et al., 2017; Wilson et al., 2015). Modelling studies have also suggested that INPs from the ocean can significantly modify the properties of mixed-phase clouds in the atmosphere, with implications for radiative forcing

20   predictions (Yun and Penner, 2013). Despite the growing evidence indicating that sea spray aerosol is an important type of INPs, our understanding of when and where sea spray aerosol is an important component of the total INP population is far from complete. Additional field measurements of INPs in marine environments would help improve our understanding of this topic.

Here we report INP measurements in the immersion mode from three coastal marine sites. Immersion freezing refers to

25   freezing initiated by INPs immersed in liquid droplets (Vali et al., 2015), and this freezing mode is considered to be the most relevant for mixed-phase clouds (Ansmann et al., 2009; de Boer et al., 2011; Westbrook and Illingworth, 2011). The three coastal marine sites investigated were Amphitrite Point, Labrador Sea, and Lancaster Sound (Fig. 1). For two of these sites (Amphitrite Point and Labrador Sea), the size distributions of INPs in the immersion mode have been reported previously (Mason et al., 2015a, 2016). In the following, we build on these previous measurements by reporting the following for all

30   three coastal marine sites: 1) the size distribution of INPs, 2) the fraction of aerosol particles acting as an INP as a function of size, and 3) the surface active site density, n_s, as a function of size. In addition, we compare the INP measurements to predictions from a recently developed global model of INP concentrations (Vergara-Temprado et al., 2017). We use this combined information to help determine if sea spray aerosol or mineral dust are the major sources of INPs at these three sites. This type of information is needed to help constrain future modeling studies of INPs and mixed-phase clouds.

2 Methods

2.1 Measurements of INP concentrations as a function of size

Concentrations of INPs as a function of size were measured with the micro-orifice uniform deposit impactor-droplet freezing technique (MOUDI-DFT; Mason et al., 2015b). This technique involves collecting size-fractionated aerosol particles on

5 hydrophobic glass slides with a micro-orifice uniform deposit impactor (MOUDI; Marple et al., 1991), and determining the freezing properties of collected aerosol particles with the droplet freezing technique (DFT). Details are given below.

2.1.1 Aerosol particle sampling with a MOUDI

A MOUDI (model 110R or 120R; MSP Corp., Shoreview, MN, USA) was used to collect size-fractionated aerosol particles. Aerosol particles were sampled at a flow rate of 30 L min^{-1}. The MOUDI has eleven stages, and each stage consists of a

10 nozzle plate and an impaction plate. Aerosol particles were collected by inertial impaction onto hydrophobic glass slides (HR3-215; Hampton Research, USA) positioned on top of each impaction plate. Custom substrate holders were used to position the glass slides within the MOUDI. See Mason et al. (2015b) for details on the substrate holders. Only Stages 2-8 of the MOUDI were analyzed for this study, corresponding to aerodynamic diameters of 5.6-10 µm, 3.2-5.6 µm, 1.8-3.2 µm, 1.0-1.8 µm, 0.56-1.0 µm, 0.32-0.56 µm and 0.18-0.32 µm, respectively, where the bounds are 50 % cut-off efficiencies

15 (Marple et al., 1991).

Particle rebound from the substrate is an issue when sampling particles with an inertial impactor. Rebound occurs when the kinetic energy of the particles striking the impactor substrate exceeds the adhesion and dissipation energies at impact (Bateman et al., 2014). Rebound can alter the number concentration and size distribution of the INPs determined with the MOUDI-DFT. Previous work has shown that particle rebound can be reduced when relative humidity (RH) is above 70 %

20 (Bateman et al., 2014; Chen et al., 2011; Fang et al., 1991). In addition, good agreement between INP concentrations measured by the MOUDI-DFT and INP concentrations measured by a continuous flow diffusion chamber (a technique that is not susceptible to rebound) has been observed in previous field campaigns when the RH of the sampled aerosol stream was as low as 40-45% (DeMott et al., 2017; Mason et al., 2015b).

2.1.2 Droplet freezing experiments

25 The freezing properties of the collected aerosol particles were determined using the DFT (Iannone et al., 2011; Mason et al., 2015b; Wheeler et al., 2015). Briefly, the hydrophobic glass slides with the collected particles were placed in a temperature- and humidity-controlled flow cell coupled to an optical microscope (Axiolab; Zeiss, Oberkochen, Germany). Water droplets with diameters of approximately 50-150 µm were condensed on the particles by increasing the humidity to above water saturation. After the condensation of water droplets on the particles, the flow cell was cooled down to -40 ºC at a rate of -10

30 ºC min^{-1} while images of the droplets were recorded. The images were then used to determine the freezing temperature for each droplet. From the freezing temperatures, INP number concentrations were calculated using the following equation:

$$[INPs(T)] = -ln\left(\frac{N_u(T)}{N_0}\right) N_0 \left(\frac{A_{deposit}}{A_{DFT}V}\right) f_{nu,1\,mm} f_{nu,0.25-1\,mm},$$ (1)

where $[INPs(T)]$ is the INP number concentration at temperature T; $N_u(T)$ is the number of unfrozen droplets at temperature T; N_0 is the total number of droplets analyzed within an experiment; $A_{deposit}$ is the total area of the sample deposit on each MOUDI impaction plate; A_{DFT} is the area analyzed in the droplet freezing experiment; V is the total volume

5   of air sampled by the MOUDI; $f_{nu,1\,mm}$ and $f_{nu,0.25-0.1\,mm}$ are correction factors for the non-uniformity of particle concentrations across the sample deposit at a scale of 1 mm and 0.25-0.1 mm, respectively. The values of $f_{nu,1\,mm}$ and $f_{nu,0.25-0.1\,mm}$ are given in Table S1 in the Supplement. Equation (1) accounts for the possibility of multiple INPs in one droplet (Vali, 1971). See Mason et al. (2015b) for further details.

2.2 Measurements of aerosol particle number and surface area size distributions

10   The combination of an aerodynamic particle sizer (APS) and a scanning mobility particle sizer (SMPS) were used to measure the aerosol number and surface area as a function of size. The APS (model 3321, TSI, Shoreview, MN, USA) measures diameters using the time-of-flight technique (Baron, 1986). At all three sites, the APS was operated with a sample flow of 1 L min⁻¹ and a sheath flow of 4 L min⁻¹. The aerodynamic diameter range measured by the APS was 0.54-20 µm. The SMPS measures diameters based on the mobility of a particle in an electric field (Asbach et al., 2009; Hoppel, 1978). At

15   Amphitrite Point, the SMPS (model 3936, TSI) was operated at 0.57 L min⁻¹ aerosol flow with 2 L min⁻¹ sheath flow, and was used to measure particles with mobility diameters from 18.4 to 930.6 nm. At Labrador Sea and Lancaster Sound, the SMPS (model 3034, TSI) was operated at 1 L min⁻¹ sample flow rate with 4 L min⁻¹ sheath flow and was used to measure particles with mobility diameters from 10 to 487 nm. The sampling condition and strategy is discussed below for each site.

2.3 Locations of sampling

20   Sampling occurred at three coastal marine sites: Amphitrite Point (48.92º N, 125.54º W) on Vancouver Island in British Columbia, Labrador Sea (54.59º N, 55.61º W) off the coast of Newfoundland and Labrador, and Lancaster Sound (74.26º N, 91.46º W) between Devon Island and Somerset Island in Nunavut, Canada (Fig. 1 and Table 1). All measurements were conducted as part of the NETwork on Climate and Aerosols: addressing key uncertainties in Remote Canadian Environments (NETCARE). Average sampling times, ambient RH values, ambient temperatures, and wind speed during sampling are

25   summarized in Table 1. Additional details about the three coastal marine sites are given below.

2.3.1 Amphitrite Point

Measurements at Amphitrite Point were carried out at a marine boundary layer site operated by Environment and Climate Change Canada, BC Ministry of the Environment, and Metro Vancouver. This site, which is frequently influenced by marine background air (McKendry et al., 2014), is located on the west coast of Vancouver Island, British Columbia, Canada and is

approximately 2.3 km south of the town of Ucluelet (population 1627), with the Pacific Ocean to its west and south, and Barkley Sound to its southeast and east.

MOUDI samples were collected from 8 to 27 August 2013 (18 day samples, 16 night samples) as part of a larger campaign that focused on cloud condensation nuclei and INPs at a marine coastal environment (Ladino et al., 2016; Mason et al.,

5 2015a, 2015b; Yakobi-Hancock et al., 2014). The average INP concentrations as a function of size for the entire campaign have been reported previously as well as the INP concentrations for each sample (Mason et al., 2015a). In the following we focus on a subset of these measurements (12 day samples, 11 night samples) corresponding to the time period when MOUDI-DFT, APS, and SMPS data are all available.

The MOUDI, APS, and SMPS were located within a mobile trailer (herein referred to as the NETCARE trailer) that was

10 approximately 100 m from the rocky shoreline of the Pacific Ocean, separated by a narrow row of trees and shrubs approximately 2-10 m in height (Mason et al., 2015a). Aerosol particles were sampled through louvered total suspended particulate (TSP) inlets (Mesa Labs Inc., Butler, NJ, USA) that were approximately 25 m above sea level. The MOUDI and APS sampled directly from ambient air without drying, whereas the SMPS sampled ambient air through a diffusion dryer. After MOUDI samples were collected, they were stored in petri dishes at room temperature and analyzed for INP

15 concentrations within 24 h of collection.

Meteorological parameters were measured at a lighthouse that was approximately halfway between the NETCARE trailer and the Pacific Ocean. The ambient temperature and RH were measured with an HMP45C probe (Campbell Scientific, Logan, UT, USA). Wind speed was determined by a model 05305L Wind Monitor (R. M. Young, Traverse City, Michigan, USA). The temperature and RH within the NETCARE trailer were monitored using a temperature/RH sensor probe (Acurite

20 00891W3). The average temperature inside the NETCARE trailer during INP sampling period was 25 ºC, compared to an average ambient temperature of 14 ºC. As a result, the average RH of the air sampled by the MOUDI and APS inside the trailer was lower than ambient RH. Based on the average ambient temperature and RH and average temperature within the trailer, the average RH in the sampling line for the MOUDI and APS was approximately 50%. For the SMPS, the average RH in the sampling line was usually below 2%, since a dryer was used (the silica was changed every 24h) prior to sampling

25 with the SMPS.

2.3.2 Labrador Sea and Lancaster Sound

Measurements at the Labrador Sea and Lancaster Sound were carried out onboard the Canadian Coast Guard Service (CCGS) vessel Amundsen. Amundsen serves as both an icebreaker for shipping lanes and a research vessel. The APS and MOUDI were located next to each other on top of the bridge of this vessel. Sampling occurred through louvered TSP inlets that were

30 approximately 15 m above sea level. The SMPS was positioned behind the bridge, approximately 20 m away from the APS and MOUDI, and sampled aerosol particles through 3/8" outside diameter stainless steel tube with an inverted U-shaped inlet that was approximately 15 m above sea level. Meteorological parameters were measured with sensors on a tower deployed on the foredeck of the Amundsen. Wind speed and direction were monitored at a height of 16 m above sea surface using a

conventional propeller anemometer (RM Young Co. model 15106MA). Temperature and RH were measured using an RH/Temperature probe (Vaisala model HMP45C212) housed in a vented sunshield.

One MOUDI sample was collected on 11 July 2014 while in the Labrador Sea off the coast of Newfoundland and Labrador. Results of this sample have been reported in Mason et al. (2016). A second MOUDI sample was collected on 20 July 2014

5   while in the Lancaster Sound between Devon Island and Somerset Island. When the two MOUDI samples were collected, the apparent wind direction was ±90º of the bow and the wind speed was > 5 knots (9.26 km h^{-1}), suggesting that ship emissions did not influence the samples (Johnson et al., 2008). After collection, the samples were vacuum-sealed and stored in a 4 ºC fridge for 45-46 days prior to analysis.

2.4 Conversion of mobility diameter to aerodynamic diameter and corrections for hygroscopic growth

10   A dryer was not used prior to sampling INPs with the MOUDI, hence INP size distributions reported in this paper correspond to the RH and temperatures during sampling and the sizes are reported in aerodynamic diameter. A dryer was also not used when sampling with the APS, and hence the same applies to the APS data reported here. On the other hand, the SMPS measured mobility diameter rather than aerodynamic diameter and a dryer was used prior to sampling with the SMPS at the Amphitrite Point site. To allow comparison between the INP data, APS data and SMPS data, all the SMPS data has

15   been converted to aerodynamic diameter, and for the case where a dryer was used prior to sampling with the SMPS, a hygroscopic growth factor was applied to the SMPS data to convert the dry diameters to wet diameters at the corresponding RH and temperatures during sampling (See Sect. S1-S2 in the Supplement).

2.5 Back trajectory analysis

For each MOUDI sample collected for INP analysis, a 3-day back trajectory was calculated using the HYSPLIT4 (Hybrid

20   Single-Particle Lagrangian Integrated Trajectory) model of the NOAA Air Resources Laboratory (Stein et al., 2015). The GDAS (Global Data Assimilation System) 1 degree meteorological data was used as input. Back trajectories were initiated at the beginning of each MOUDI sampling period and at every hour until the end of the sampling period. The initiating height was the same as the height of the MOUDI sampling inlets as mentioned in Sect. 2.3. Back trajectories were also initiated at heights of 50 m and 150 m a.g.l. for each location to determine if the trajectories were sensitive to the height of initiation.

25   **2.6 Global model of INP concentrations**

A global model of INP concentrations relevant for mixed-phase clouds was used to predict concentrations of INPs at the three sampling sites (Vergara-Temprado et al., 2017). The model considers ice nucleation by K-feldspar, associated with desert dust, and marine organics, associated with sea spray aerosol, as INPs. In this model (GLOMAP-mode) aerosol number and mass concentration of several aerosol species are simulated in seven lognormal modes (3 insoluble and 4 soluble). The

30   model has a horizontal resolution of 2.8 x 2.8 degrees with 30 vertical levels and it is run for the year 2001 with meteorological fields from the European Centre for Medium-Range Weather Forecasts (ECMWF). The aerosol components

are emitted internally mixed with the species of their mode and several aerosol microphysical processes including new particle formation, particle growth, dry deposition and wet scavenging are represented (Mann et al., 2014). The INP concentrations are determined using a laboratory-based temperature-dependent density of active sites (active sites per unit surface area) for K-feldspar (Atkinson et al., 2013) and a parameterization for marine organics based on the INP content of

5   microlayer samples (expressed as sites per unit mass of organic carbon) (Wilson et al., 2015) following the method shown in Vergara Temprado et al. (2017) Appendix 2.

To predict INP concentrations at the three coastal marine sites, we used the output of the model for the grid cells that overlapped with the measurement locations. We calculated the mean concentrations of INPs from K-feldspar and marine organics for the months when measurements were made. For the simulations at Amphitrite Point, Labrador Sea, and

10   Lancaster Sound, the months of August, July, and July were used, respectively.

3 Results and discussion

3.1 Air mass sources from back trajectories

Figure 2 shows the 3-day back trajectories initiated for every hour during MOUDI sampling at the three sites. The initiation heights were the same as the MOUDI sampling inlet heights. Similar results were obtained using initiation heights of 50 m

15   and 150 m a.g.l. (see Fig. S1-S2 in the Supplement). When considering all the back trajectories, at Amphitrite Point, 94 % of the time was spent over ocean, at Labrador Sea, 40 % of the time was spent over ocean, and at Lancaster Sound, 63% of the time was spent over ocean. The rest of the time was spent over land. The trajectories suggest that marine and terrestrial sources of INPs may be important. Long-range transport of INPs from sources more than three days away are also possible.

3.2 INP concentrations as a function of size

20   In Fig. 3, the average INP number concentration is plotted as a function of size for the freezing temperatures of -15 ºC, -20 ºC, and -25 ºC. These three temperatures were chosen because freezing events were rare at temperatures warmer than -15 ºC, and for some MOUDI stages all the droplets were frozen at temperatures lower than -25 ºC, making calculations of INP concentrations using Eq. (1) not possible at temperatures lower than -25 ºC. Mason et al. (2015a) previously reported the average INP number concentrations as a function of size at Amphitrite Point for the time period of 6-27 August 2013. Here

25   we report the average INP number concentrations as a function of size at the same site for a subset of the measurements from Mason et al. (2015a) when both APS and SMPS data were available. Not surprisingly, the results shown here are very similar to the results shown by Mason et al. (2015a). The result for Labrador Sea shown in Fig. 3 has also been reported in Mason et al. (2016), while the result for Lancaster Sound is new and represents the first report of INP concentrations as a function of size in the Arctic marine boundary layer. Lancaster Sound had the lowest INP concentrations among the three

30   sites with average concentrations of INPs of 0 L^{-1}, 0.16 L^{-1}, and 0.67 L^{-1} for the freezing temperatures of -15 ºC, -20 ºC, and -25 ºC, respectively. These numbers are consistent with several previous measurements reported in the Arctic. For example,

Mason et al. (2016) reported the following mean concentrations at a surface site in Alert, Nunavut: 0.05 L^{-1}, 0.22 L^{-1} and 0.99 L^{-1} for freezing temperatures of -15 ºC, -20 ºC, and -25 ºC, respectively. Bigg (1996) reported mean INP concentration of 0.01 L^{-1} at -15 ºC on an icebreaker in the Arctic. Fountain and Ohtake (1985) measured mean INP concentrations of 0.17 L^{-1} at -20 ºC at a surface site in Barrow, Alaska.

5   At Amphitrite Point and Labrador Sea, the majority of INPs measured were > 1 µm in diameter at all the temperatures studied. At Lancaster Sound, the majority of INPs were also > 1 µm at -25 ºC. At -15 ºC, the concentrations of INPs were not above detection limit at any of the sizes, while at -20 ºC, freezing was only observed for sizes between 0.56 and 1 µm.

3.3 Size distributions of ambient aerosols

As mentioned above, the concentrations of aerosol number and surface area as a function of size were determined from
10   measurements with a SMPS and an APS. The results are shown in Fig. 4. For the size range shown, the average total number concentrations were 598 cm^{-3}, 303 cm^{-3}, and 404 cm^{-3} for Amphitrite Point, Labrador Sea, and Lancaster Sound, respectively. For the three sites studied, < 1 % of the number concentration was supermicron in diameter, and < 45 % of the surface area concentration was supermicron in diameter. The concentrations and size distributions reported here are, in general, consistent with previous measurements of ambient aerosol size distributions at marine boundary layer sites (DeMott
15   et al., 2016; O'Dowd et al., 2001).

3.4 Ice-nucleating efficiency on a per number basis

The ice-nucleating efficiency on a per number basis is represented as the fraction of aerosol particles acting as an INP. Shown in Fig. 5 is the fraction of aerosol particles acting as an INP as a function of size. To generate Fig. 5, first the aerosol number concentrations (Fig. 4a) was binned using the same bin widths as the MOUDI, resulting in the total aerosol number
20   concentration in each size bin (Fig. S3a). Then the INP concentration (Fig. 3) was divided by the aerosol number concentration (Fig. S3a). Figure 5 shows that the fraction of particles acting as an INP is strongly dependent on the size. For Amphitrite Point and Labrador Sea, and for diameters of around 0.2 µm, approximately 1 in 10^6 particles acted as an INP at -25 ºC. On the other hand, at the same sites and for diameters of around 8 µm, approximately 1 in 10 particles acted as an INP at -25 ºC. A similar trend may be present at Lancaster Sound, but at the smaller sizes investigated, the concentrations of INPs
25   were below detection limit. The results in Fig. 5 show that the large particles at the three sites studied are extremely efficient at nucleating ice, and as a result, even though the number concentration of large particles might be small in the atmosphere, they can make an important contribution to the total INP number concentrations.

The strong dependence on the size shown in Fig. 5 is consistent with the small number of previous studies that investigated the fraction of aerosol particles acting as an INP as a function of size. Berezinski et al. (1988) studied INPs collected at 100-
30   500 m above ground level in the southern part of the European territory of the former USSR. At a freezing temperature of -20 ºC and for a diameter of 0.1 µm, approximately 1 in 10^5 particles acted as an INP, while for a diameter of 10 µm approximately 1 in 100 particles acted as an INP. Huffman et al. (2013) studied INPs collected at a semi-arid pine forest in

Colorado, United States. At a freezing temperature of -15 ºC and for a diameter of 2 µm approximately 1 in 10^3 particles acted as an INP, while at the same freezing temperature but for a diameter of 10 µm, more than 1 in 100 particles acted as an INP.

3.5 Ice-nucleating efficiency on a per surface area basis

5 The ice-nucleating efficiency on a per surface area basis is represented as the surface active site density, n_s (Connolly et al., 2009; Hoose and Möhler, 2012). Shown in Fig. 6 is the measured n_s as a function of size. To generate Fig. 6, first the aerosol surface area concentration (Fig. 4b) was binned using the same bin widths as the MOUDI, resulting in the total aerosol surface area concentration in each size bin (Fig. S3b). The INP concentration (Fig. 3) was then divided by the aerosol surface area concentration (Fig. S3b). Figure. 6 shows that n_s is dependent on the size, with the larger particles being more efficient

10 at nucleating ice. For Amphitrite Point and Labrador Sea, at a freezing temperature of -25 ºC, n_s was two orders of magnitude higher for 8 µm particles compared to 0.2 µm particles.

To determine whether sea spray aerosol or mineral dust are the major sources of INPs at the three sites, the measured n_s values were compared to n_s values of sea spray aerosol and mineral dust at -15 ºC, -20 ºC, and -25 ºC, respectively (Fig. 7). The n_s values of sea spray aerosol in Fig. 7 are from field studies in the marine boundary layer and laboratory studies of sea

15 spray aerosol as reported in DeMott et al. (2016). Specifically, the data in Fig. 1A in DeMott et al. (2016) were re-plotted and fitted using linear regression (see Fig. S4 in the Supplement). Since the reported n_s values in DeMott et al. (2016) correspond to dry conditions, these values should be considered as upper limits to the n_s values for sea spray aerosol exposed to high RH values. Figure 7 shows that the n_s values of sea spray aerosol are smaller than the measured n_s values in the supermicron range at all freezing temperatures at Amphitrite Point. This is also the case for Labrador Sea at freezing

20 temperatures of -20 and -25 ºC. For Lancaster Sound, the n_s values of sea spray aerosol are smaller than the measured n_s values for sizes of 5.6-10 µm and a freezing temperature of -25 ºC. These combined results suggest that sea spray aerosol was not the major contributor to the supermicron INP population at Amphitrite Point and Labrador Sea, and not a contributor to the largest INPs (> 5.6 µm in size) observed at Lancaster Sound.

The n_s values of mineral dust particles shown in Fig. 7 are based on laboratory measurements with five different dust

25 samples: Asian dust, Saharan dust, Canary Island dust, Israel dust, and Arizona test dust (Niemand et al., 2012). Specifically, the data in Fig. 6 in Niemand et al. (2012) were re-plotted and fitted using linear regression (see Fig. S5 in the Supplement). Figure 7 shows that the n_s values for mineral dust are greater than or equal to the measured n_s values at all three sites. These results suggest that mineral dust could be a possible source of the supermicron INPs at the three sites studied. However, these results do not confirm mineral dust as the major contributor of supermicron INPs nor do they rule out other types of

30 particles as the major contributor of supermicron INPs.

3.6 Comparison between measured and simulated INP concentrations

Shown in Fig. 8 is a comparison between the measured INP concentrations and the simulated INP concentrations at the three sites using a global model of INP concentrations based on the ice nucleation of K-feldspar and marine organics. When considering only marine organics as INPs in the model, predicted INP concentrations are less than measured INP
5   concentrations in all cases except for Amphitrite Point at a freezing temperature of -25 ºC. This suggests that sea spray aerosol is not the dominant source of INPs at the three coastal marine sites studied for all three temperatures, which is consistent with conclusions reached in Sect. 3.5. When considering only K-feldspar, associated with desert dusts, as INPs in the model, the predicted INP concentrations at -25 ºC are consistent with the measurements at all three sites, but at -15 ºC and -20 ºC the predicted INP concentrations are less than measured. When considering both marine organics and K-feldspar
10   as INPs in the model the predicted INP concentrations at -25 ºC are consistent with measurements, but at warmer temperatures the predicted INPs are still less than measured. These results suggest that the model could be missing a source of INPs that are active at temperatures warmer than -25 ºC, consistent with the conclusion that has been drawn in Vergara Temprado et al. (2017) based on other sites. Possible sources missing in the model that could explain the high-temperature INPs include bacteria, fungal material, agricultural dust or biological nanoscale fragments attached to mineral dust particles
15   (Fröhlich-Nowoisky et al., 2015; Garcia et al., 2012; Haga et al., 2013; Mason et al., 2015a; Möhler et al., 2008; Morris et al., 2004, 2013, O'Sullivan et al., 2014, 2015, 2016; Spracklen and Heald, 2014; Tobo et al., 2013, 2014).
Recently Mason et al. (2015a) investigated the source of INPs at Amphitrite Point using correlations between INP number concentrations, atmospheric particles and meteorological conditions. Correlations between INP number concentrations and marine aerosol and marine biological activities were not statistically significant. On the other hand, a strong correlation was
20   observed between INP concentrations and fluorescent bioparticles, suggesting biological particles from terrestrial sources were likely a dominant source of INPs. These results are consistent and complementary to the studies presented above.

4 Summary and conclusions

The INP number concentrations in the immersion freezing mode as a function of size were determined at three coastal marine sites in Canada: Amphitrite Point (48.92º N, 125.54º W), Labrador Sea (54.59º N, 55.61º W), and Lancaster Sound
25   (74.26º N, 91.46º W). The result for Lancaster Sound is the first report of INP number concentrations as a function of size in the Arctic marine boundary layer. The freezing efficiencies of aerosol particles as a function of size were then investigated by combing the size-resolved concentrations of INPs and the size distributions of aerosol number and surface area. We found that the fraction of particles acting as an INP is strongly dependent on the size. At -25 ºC and for Amphitrite Point and Labrador Sea, approximately 1 in 10^6 particles acted as an INP at diameters around 0.2 µm, while approximately 1 in 10
30   particles acted as an INP at diameters around 8 µm. We also found that the surface active site density, n_s, is dependent on the size. At -25 ºC and for Amphitrite Point and Labrador Sea, n_s was two orders of magnitude higher for 8 µm particles compared to 0.2 µm particles.

Sea spray aerosol and mineral dust were investigated as the possible sources of INPs. Sea spray aerosol was not the major source of INPs based on comparison of the measurements with the n_s values of sea spray aerosol, and the INP concentrations predicted by a global model. On the other hand, the mineral dust may be the main source of INPs at the three sites and at a freezing temperature of -25 ºC based on the comparison of the measured INP concentrations with the predictions of a global

5   model. However, the under-prediction of the INP concentrations at -15 ºC and -20 ºC suggests the existence of other possible sources of INPs such as biological particles or agricultural dust. Ideally, similar studies in the future will also include information on the aerosol chemical composition to confirm conclusions reached in the current study.

References:

Alpert, P. A., Aller, J. Y. and Knopf, D. A.: Ice nucleation from aqueous NaCl droplets with and without marine diatoms,
10   Atmos. Chem. Phys., 11(12), 5539–5555, doi:10.5194/acp-11-5539-2011, 2011a.

Alpert, P. A., Aller, J. Y. and Knopf, D. A.: Initiation of the ice phase by marine biogenic surfaces in supersaturated gas and supercooled aqueous phases, Phys. Chem. Chem. Phys., 13(44), 19882, doi:10.1039/c1cp21844a, 2011b.

Andreae, M. O. and Rosenfeld, D.: Aerosol-cloud-precipitation interactions. Part 1. The nature and sources of cloud-active aerosols, Earth-Science Rev., 89(1–2), 13–41, doi:10.1016/j.earscirev.2008.03.001, 2008.

15   Ansmann, A., Tesche, M., Seifert, P., Althausen, D., Engelmann, R., Fruntke, J., Wandinger, U., Mattis, I. and Müller, D.: Evolution of the ice phase in tropical altocumulus: SAMUM lidar observations over Cape Verde, J. Geophys. Res., 114(D17), D17208, doi:10.1029/2008JD011659, 2009.

Asbach, C., Kaminski, H., Fissan, H., Monz, C., Dahmann, D., Mülhopt, S., Paur, H. R., Kiesling, H. J., Herrmann, F., Voetz, M. and Kuhlbusch, T. A. J.: Comparison of four mobility particle sizers with different time resolution for stationary
20   exposure measurements, J. Nanoparticle Res., 11(7), 1593–1609, doi:10.1007/s11051-009-9679-x, 2009.

Atkinson, J. D., Murray, B. J., Woodhouse, M. T., Whale, T. F., Baustian, K. J., Carslaw, K. S., Dobbie, S., O'Sullivan, D. and Malkin, T. L.: The importance of feldspar for ice nucleation by mineral dust in mixed-phase clouds, Nature, 498(7454), 355–358, doi:10.1038/nature12278, 2013.

Baron, P. A.: Calibration and use of the aerodynamic particle sizer (APS 3300), Aerosol Sci. Technol., 5(1), 55–67,
25   doi:10.1080/02786828608959076, 1986.

Bateman, A. P., Belassein, H. and Martin, S. T.: Impactor apparatus for the study of particle rebound: Relative humidity and capillary forces, Aerosol Sci. Technol., 48(1), 42–52, doi:10.1080/02786826.2013.853866, 2014.

Berezinski, N. A., Stepanov, G. V. and Khorguani, V. G.: Ice-forming activity of atmospheric aerosol particles of different sizes, Atmos. Aerosols Nucleation, 309, 709–712, 1988.

30   Bigg, E. K.: Ice Nucleus Concentrations in Remote Areas, J. Atmos. Sci., 30(6), 1153–1157, 1973.

Bigg, E. K.: Ice forming nuclei in the high Arctic, Tellus B, 48(2), 223–233, doi:10.1034/j.1600-0889.1996.t01-1-00007.x, 1996.

de Boer, G., Morrison, H., Shupe, M. D. and Hildner, R.: Evidence of liquid dependent ice nucleation in high-latitude stratiform clouds from surface remote sensors, Geophys. Res. Lett., 38(1), n/a-n/a, doi:10.1029/2010GL046016, 2011.

Boose, Y., Welti, A., Atkinson, J., Ramelli, F., Danielczok, A., Bingemer, H. G., Plötze, M., Sierau, B., Kanji, Z. A. and Lohmann, U.: Heterogeneous ice nucleation on dust particles sourced from nine deserts worldwide - Part 1: Immersion freezing, Atmos. Chem. Phys., 16(23), 15075–15095, doi:10.5194/acp-16-15075-2016, 2016a.

Boose, Y., Sierau, B., Isabel García, M., Rodríguez, S., Alastuey, A. A., Linke, C., Schnaiter, M., Kupiszewski, P., Kanji, Z. A., Lohmann, U., Isabel Garc??a, M., Rodr??guez, S., Alastuey, A. A., Linke, C., Schnaiter, M., Kupiszewski, P., Kanji, Z. A., Lohmann, U., García, M. I., Rodríguez, S., Alastuey, A. A., Linke, C., Schnaiter, M., Kupiszewski, P., Kanji, Z. A. and Lohmann, U.: Ice nucleating particles in the Saharan Air Layer, Atmos. Chem. Phys., 16(14), 9067–9087, doi:10.5194/acp-16-9067-2016, 2016b.

Broadley, S. L., Murray, B. J., Herbert, R. J., Atkinson, J. D., Dobbie, S., Malkin, T. L., Condliffe, E. and Neve, L.: Immersion mode heterogeneous ice nucleation by an illite rich powder representative of atmospheric mineral dust, Atmos. Chem. Phys., 12(1), 287–307, doi:10.5194/acp-12-287-2012, 2012.

Burrows, S. M., Hoose, C., Pöschl, U. and Lawrence, M. G.: Ice nuclei in marine air: Biogenic particles or dust?, Atmos. Chem. Phys., 13(1), 245–267, doi:10.5194/acp-13-245-2013, 2013.

Chen, S. C., Tsai, C. J., Chen, H. D., Huang, C. Y. and Roam, G. D.: The Influence of Relative Humidity on Nanoparticle Concentration and Particle Mass Distribution Measurements by the MOUDI, Aerosol Sci. Technol., 45(5), 596–603, doi:10.1080/02786826.2010.551557, 2011.

Connolly, P. J., Möhler, O., Field, P. R., Saathoff, H., Burgess, R., Choularton, T. and Gallagher, M.: Studies of heterogeneous freezing by three different desert dust samples, Atmos. Chem. Phys., 9(8), 2805–2824, doi:10.5194/acp-9-2805-2009, 2009.

Cziczo, D. J. and Abbatt, J. P. D.: Ice nucleation in NH4HSO4, NH4NO3, and H2SO4 aqueous particles: Implications for circus cloud formation, Geophys. Res. Lett., 28(6), 963–966, doi:10.1029/2000GL012568, 2001.

DeMott, P. J., Sassen, K., Poellot, M. R., Baumgardner, D., Rogers, D. C., Brooks, S. D., Prenni, A. J. and Kreidenweis, S. M.: African dust aerosols as atmospheric ice nuclei, Geophys. Res. Lett., 30(14), 26–29, doi:10.1029/2003GL017410, 2003.

DeMott, P. J., Hill, T. C. J., McCluskey, C. S., Prather, K. A., Collins, D. B., Sullivan, R. C., Ruppel, M. J., Mason, R. H., Irish, V. E., Lee, T., Hwang, C. Y., Rhee, T. S., Snider, J. R., McMeeking, G. R., Dhaniyala, S., Lewis, E. R., Wentzell, J. J. B., Abbatt, J., Lee, C., Sultana, C. M., Ault, A. P., Axson, J. L., Diaz Martinez, M., Venero, I., Santos-Figueroa, G., Stokes, M. D., Deane, G. B., Mayol-Bracero, O. L., Grassian, V. H., Bertram, T. H., Bertram, A. K., Moffett, B. F. and Franc, G. D.: Sea spray aerosol as a unique source of ice nucleating particles, Proc. Natl. Acad. Sci., 113(21), 5797–5803, doi:10.1073/pnas.1514034112, 2016.

DeMott, P. J., Hill, T. C. J., Petters, M. D., Bertram, A. K., Tobo, Y., Mason, R. H., Suski, K. J., McCluskey, C. S., Levin, E. J. T., Schill, G. P., Boose, Y., Rauker, A. M., Miller, A. J., Zaragoza, J., Rocci, K., Rothfuss, N. E., Taylor, H. P., Hader, J. D., Chou, C., Huffman, J. A., Pöschl, U., Prenni, A. J. and Kreidenweis, S. M.: Comparative measurements of ambient

atmospheric concentrations of ice nucleating particles using multiple immersion freezing methods and a continuous flow diffusion chamber, Atmos. Chem. Phys., 17(18), 11227–11245, doi:10.5194/acp-17-11227-2017, 2017.

Eastwood, M. L., Cremel, S., Gehrke, C., Girard, E. and Bertram, A. K.: Ice nucleation on mineral dust particles: Onset conditions, nucleation rates and contact angles, J. Geophys. Res., 113(D22), D22203, doi:10.1029/2008JD010639, 2008.

5 Fang, C. P., McMurry, P. H., Marple, V. A. and Rubow, K. L.: Effect of Flow-induced Relative Humidity Changes on Size Cuts for Sulfuric Acid Droplets in the Microorifice Uniform Deposit Impactor (MOUDI), Aerosol Sci. Technol., 14(2), 266–277, doi:10.1080/02786829108959489, 1991.

Field, P. R., Möhler, O., Connolly, P., Krämer, M., Cotton, R., Heymsfield, A. J., Saathoff, H. and Schnaiter, M.: Some ice nucleation characteristics of Asian and Saharan desert dust, Atmos. Chem. Phys., 6(10), 2991–3006, doi:10.5194/acp-6-
10 2991-2006, 2006.

Fountain, A. G. and Ohtake, T.: Concentrations and Source Areas of Ice Nuclei in the Alaskan Atmosphere, J. Clim. Appl. Meteorol., 24(4), 377–382, doi:10.1175/1520-0450(1985)024<0377:CASAOI>2.0.CO;2, 1985.

Fröhlich-Nowoisky, J., Hill, T. C. J., Pummer, B. G., Yordanova, P., Franc, G. D. and Pöschl, U.: Ice nucleation activity in the widespread soil fungus *Mortierella alpina*, Biogeosciences, 12(4), 1057–1071, doi:10.5194/bg-12-1057-2015, 2015.

15 Garcia, E., Hill, T. C. J., Prenni, A. J., DeMott, P. J., Franc, G. D. and Kreidenweis, S. M.: Biogenic ice nuclei in boundary layer air over two U.S. High Plains agricultural regions, J. Geophys. Res. Atmos., 117(D18), D18209, doi:10.1029/2012JD018343, 2012.

Haga, D. I., Iannone, R., Wheeler, M. J., Mason, R., Polishchuk, E. A., Fetch, T., Van Der Kamp, B. J., McKendry, I. G. and Bertram, A. K.: Ice nucleation properties of rust and bunt fungal spores and their transport to high altitudes, where they can
20 cause heterogeneous freezing, J. Geophys. Res. Atmos., 118(13), 7260–7272, doi:10.1002/jgrd.50556, 2013.

Harrison, A. D., Whale, T. F., Carpenter, M. A., Holden, M. A., Neve, L., O'Sullivan, D., Vergara Temprado, J. and Murray, B. J.: Not all feldspars are equal: a survey of ice nucleating properties across the feldspar group of minerals, Atmos. Chem. Phys., 16(17), 10927–10940, doi:10.5194/acp-16-10927-2016, 2016.

Hartmann, S., Wex, H., Clauss, T., Augustin-Bauditz, S., Niedermeier, D., Rösch, M. and Stratmann, F.: Immersion
25 Freezing of Kaolinite: Scaling with Particle Surface Area, J. Atmos. Sci., 73(1), 263–278, doi:10.1175/JAS-D-15-0057.1, 2016.

Hiranuma, N., Augustin-Bauditz, S., Bingemer, H., Budke, C., Curtius, J., Danielczok, A., Diehl, K., Dreischmeier, K., Ebert, M., Frank, F., Hoffmann, N., Kandler, K., Kiselev, A., Koop, T., Leisner, T., Möhler, O., Nillius, B., Peckhaus, A., Rose, D., Weinbruch, S., Wex, H., Boose, Y., DeMott, P. J., Hader, J. D., Hill, T. C. J., Kanji, Z. A., Kulkarni, G., Levin, E.
30 J. T., McCluskey, C. S., Murakami, M., Murray, B. J., Niedermeier, D., Petters, M. D., O'Sullivan, D., Saito, A., Schill, G. P., Tajiri, T., Tolbert, M. A., Welti, A., Whale, T. F., Wright, T. P. and Yamashita, K.: A comprehensive laboratory study on the immersion freezing behavior of illite NX particles: a comparison of 17 ice nucleation measurement techniques, Atmos. Chem. Phys., 15(5), 2489–2518, doi:10.5194/acp-15-2489-2015, 2015.

Hoose, C. and Möhler, O.: Heterogeneous ice nucleation on atmospheric aerosols: a review of results from laboratory experiments, Atmos. Chem. Phys., 12(20), 9817–9854, doi:10.5194/acp-12-9817-2012, 2012.

Hoose, C., Kristjánsson, J. E., Chen, J.-P. and Hazra, A.: A Classical-Theory-Based Parameterization of Heterogeneous Ice Nucleation by Mineral Dust, Soot, and Biological Particles in a Global Climate Model, J. Atmos. Sci., 67(8), 2483–2503,
5   doi:10.1175/2010JAS3425.1, 2010.

Hoppel, W. A.: Determination of the aerosol size distribution from the mobility distribution of the charged fraction of aerosols, J. Aerosol Sci., 9(1), 41–54, doi:10.1016/0021-8502(78)90062-9, 1978.

Huffman, J. A., Prenni, A. J., DeMott, P. J., Pöhlker, C., Mason, R. H., Robinson, N. H., Fröhlich-Nowoisky, J., Tobo, Y., Després, V. R., Garcia, E., Gochis, D. J., Harris, E., Müller-Germann, I., Ruzene, C., Schmer, B., Sinha, B., Day, D. A.,
10   Andreae, M. O., Jimenez, J. L., Gallagher, M., Kreidenweis, S. M., Bertram, A. K. and Pöschl, U.: High concentrations of biological aerosol particles and ice nuclei during and after rain, Atmos. Chem. Phys., 13(13), 6151–6164, doi:10.5194/acp-13-6151-2013, 2013.

Iannone, R., Chernoff, D. I., Pringle, A., Martin, S. T. and Bertram, A. K.: The ice nucleation ability of one of the most abundant types of fungal spores found in the atmosphere, Atmos. Chem. Phys., 11(3), 1191–1201, doi:10.5194/acp-11-1191-
15   2011, 2011.

Irish, V. E., Elizondo, P., Chen, J., Chou, C., Charette, J., Lizotte, M., Ladino, L. A., Wilson, T. W., Gosselin, M., Murray, B. J., Polishchuk, E., Abbatt, J. P. D., Miller, L. A. and Bertram, A. K.: Ice-nucleating particles in Canadian Arctic sea-surface microlayer and bulk seawater, Atmos. Chem. Phys., 17(17), 10583–10595, doi:10.5194/acp-17-10583-2017, 2017.

Johnson, M. T., Liss, P. S., Bell, T. G., Lesworth, T. J., Baker, A. R., Hind, A. J., Jickells, T. D., Biswas, K. F., Woodward,
20   E. M. S. and Gibb, S. W.: Field observations of the ocean-atmosphere exchange of ammonia: Fundamental importance of temperature as revealed by a comparison of high and low latitudes, Global Biogeochem. Cycles, 22(1), GB1019, doi:10.1029/2007GB003039, 2008.

Kanji, Z. A. and Abbatt, J. P. D.: Ice Nucleation onto Arizona Test Dust at Cirrus Temperatures: Effect of Temperature and Aerosol Size on Onset Relative Humidity, J. Phys. Chem. A, 114(2), 935–941, doi:10.1021/jp908661m, 2010.

25   Klein, H., Nickovic, S., Haunold, W., Bundke, U., Nillius, B., Ebert, M., Weinbruch, S., Schuetz, L., Levin, Z., Barrie, L. A. and Bingemer, H.: Saharan dust and ice nuclei over Central Europe, Atmos. Chem. Phys., 10(21), 10211–10221, doi:10.5194/acp-10-10211-2010, 2010.

Knopf, D. A. and Koop, T.: Heterogeneous nucleation of ice on surrogates of mineral dust, J. Geophys. Res., 111(D12), D12201, doi:10.1029/2005JD006894, 2006.

30   Knopf, D. A., Alpert, P. A., Wang, B. and Aller, J. Y.: Stimulation of ice nucleation by marine diatoms, Nat. Geosci., 4(2), 88–90, doi:10.1038/ngeo1037, 2011.

Ladino, L. A., Yakobi-Hancock, J. D., Kilthau, W. P., Mason, R. H., Si, M., Li, J., Miller, L. A., Schiller, C. L., Huffman, J. A., Aller, J. Y., Knopf, D. A., Bertram, A. K. and Abbatt, J. P. D.: Addressing the ice nucleating abilities of marine aerosol:

A combination of deposition mode laboratory and field measurements, Atmos. Environ., 132, 1–10, doi:10.1016/j.atmosenv.2016.02.028, 2016.

Lohmann, U. and Feichter, J.: Global indirect aerosol effects: a review, Atmos. Chem. Phys., 5(3), 715–737, doi:10.5194/acp-5-715-2005, 2005.

5 Mann, G. W., Carslaw, K. S., Reddington, C. L., Pringle, K. J., Schulz, M., Asmi, A., Spracklen, D. V., Ridley, D. A., Woodhouse, M. T., Lee, L. A., Zhang, K., Ghan, S. J., Easter, R. C., Liu, X., Stier, P., Lee, Y. H., Adams, P. J., Tost, H., Lelieveld, J., Bauer, S. E., Tsigaridis, K., van Noije, T. P. C., Strunk, A., Vignati, E., Bellouin, N., Dalvi, M., Johnson, C. E., Bergman, T., Kokkola, H., von Salzen, K., Yu, F., Luo, G., Petzold, A., Heintzenberg, J., Clarke, A., Ogren, J. A., Gras, J., Baltensperger, U., Kaminski, U., Jennings, S. G., O'Dowd, C. D., Harrison, R. M., Beddows, D. C. S., Kulmala, M.,

10 Viisanen, Y., Ulevicius, V., Mihalopoulos, N., Zdimal, V., Fiebig, M., Hansson, H.-C., Swietlicki, E. and Henzing, J. S.: Intercomparison and evaluation of global aerosol microphysical properties among AeroCom models of a range of complexity, Atmos. Chem. Phys., 14(9), 4679–4713, doi:10.5194/acp-14-4679-2014, 2014.

Marple, V. A., Rubow, K. L. and Behm, S. M.: A Microorifice Uniform Deposit Impactor (MOUDI): Description, Calibration, and Use, Aerosol Sci. Technol., 14(4), 434–446, doi:10.1080/02786829108959504, 1991.

15 Mason, R. H., Si, M., Li, J., Chou, C., Dickie, R., Toom-Sauntry, D., Pöhlker, C., Yakobi-Hancock, J. D., Ladino, L. A., Jones, K., Leaitch, W. R., Schiller, C. L., Abbatt, J. P. D., Huffman, J. A. and Bertram, A. K.: Ice nucleating particles at a coastal marine boundary layer site: correlations with aerosol type and meteorological conditions, Atmos. Chem. Phys., 15(21), 12547–12566, doi:10.5194/acp-15-12547-2015, 2015a.

Mason, R. H., Chou, C., McCluskey, C. S., Levin, E. J. T., Schiller, C. L., Hill, T. C. J., Huffman, J. A., DeMott, P. J. and

20 Bertram, A. K.: The micro-orifice uniform deposit impactor–droplet freezing technique (MOUDI-DFT) for measuring concentrations of ice nucleating particles as a function of size: improvements and initial validation, Atmos. Meas. Tech., 8(6), 2449–2462, doi:10.5194/amt-8-2449-2015, 2015b.

Mason, R. H., Si, M., Chou, C., Irish, V. E., Dickie, R., Elizondo, P., Wong, R., Brintnell, M., Elsasser, M., Lassar, W. M., Pierce, K. M., Leaitch, W. R., MacDonald, A. M., Platt, A., Toom-Sauntry, D., Sarda-Estève, R., Schiller, C. L., Suski, K. J.,

25 Hill, T. C. J., Abbatt, J. P. D., Huffman, J. A., DeMott, P. J. and Bertram, A. K.: Size-resolved measurements of ice-nucleating particles at six locations in North America and one in Europe, Atmos. Chem. Phys., 16(3), 1637–1651, doi:10.5194/acp-16-1637-2016, 2016.

McKendry, I., Christensen, E., Schiller, C., Vingarzan, R., Macdonald, A. M. and Li, Y.: Low Ozone Episodes at Amphitrite Point Marine Boundary Layer Observatory, British Columbia, Canada, Atmosphere-Ocean, 52(3), 271–280,

30 doi:10.1080/07055900.2014.910164, 2014.

Möhler, O., Georgakopoulos, D. G., Morris, C. E., Benz, S., Ebert, V., Hunsmann, S., Saathoff, H., Schnaiter, M. and Wagner, R.: Heterogeneous ice nucleation activity of bacteria: new laboratory experiments at simulated cloud conditions, Biogeosciences, 5(5), 1425–1435, doi:10.5194/bg-5-1425-2008, 2008.

Morris, C. E., Georgakopoulos, D. G. and Sands, D. C.: Ice nucleation active bacteria and their potential role in precipitation, J. Phys. IV, 121, 87–103, doi:10.1051/jp4:2004121004, 2004.

Morris, C. E., Sands, D. C., Glaux, C., Samsatly, J., Asaad, S., Moukahel, A. R., Gonçalves, F. L. T. and Bigg, E. K.: Urediospores of rust fungi are ice nucleation active at > −10 °C and harbor ice nucleation active bacteria, Atmos. Chem.
5 Phys., 13(8), 4223–4233, doi:10.5194/acp-13-4223-2013, 2013.

Murray, B. J., Broadley, S. L., Wilson, T. W., Atkinson, J. D. and Wills, R. H.: Heterogeneous freezing of water droplets containing kaolinite particles, Atmos. Chem. Phys., 11(9), 4191–4207, doi:10.5194/acp-11-4191-2011, 2011.

Niemand, M., Möhler, O., Vogel, B., Vogel, H., Hoose, C., Connolly, P., Klein, H., Bingemer, H., DeMott, P., Skrotzki, J. and Leisner, T.: A Particle-Surface-Area-Based Parameterization of Immersion Freezing on Desert Dust Particles, J. Atmos.
10 Sci., 69(10), 3077–3092, doi:10.1175/JAS-D-11-0249.1, 2012.

O'Dowd, C. D., Becker, E. and Kulmala, M.: Mid-latitude North-Atlantic aerosol characteristics in clean and polluted air, Atmos. Res., 58(3), 167–185, doi:10.1016/S0169-8095(01)00098-9, 2001.

O'Sullivan, D., Murray, B. J., Malkin, T. L., Whale, T. F., Umo, N. S., Atkinson, J. D., Price, H. C., Baustian, K. J., Browse, J. and Webb, M. E.: Ice nucleation by fertile soil dusts: relative importance of mineral and biogenic components, Atmos.
15 Chem. Phys., 14(4), 1853–1867, doi:10.5194/acp-14-1853-2014, 2014.

O'Sullivan, D., Murray, B. J., Ross, J. F., Whale, T. F., Price, H. C., Atkinson, J. D., Umo, N. S. and Webb, M. E.: The relevance of nanoscale biological fragments for ice nucleation in clouds, Sci. Rep., 5(1), 8082, doi:10.1038/srep08082, 2015.

O'Sullivan, D., Murray, B. J., Ross, J. F. and Webb, M. E.: The adsorption of fungal ice-nucleating proteins on mineral dusts: a terrestrial reservoir of atmospheric ice-nucleating particles, Atmos. Chem. Phys., 16(12), 7879–7887,
20 doi:10.5194/acp-16-7879-2016, 2016.

Prenni, A. J., Petters, M. D., Kreidenweis, S. M., Heald, C. L., Martin, S. T., Artaxo, P., Garland, R. M., Wollny, A. G. and Pöschl, U.: Relative roles of biogenic emissions and Saharan dust as ice nuclei in the Amazon basin, Nat. Geosci., 2(6), 402–405, doi:10.1038/ngeo517, 2009.

Rosinski, J., Haagenson, P. L., Nagamoto, C. T. and Parungo, F.: Ice-forming nuclei of maritime origin, J. Aerosol Sci.,
25 17(1), 23–46, doi:10.1016/0021-8502(86)90004-2, 1986.

Rosinski, J., Haagenson, P. L., Nagamoto, C. T., Quintana, B., Parungo, F. and Hoyt, S. D.: Ice-forming nuclei in air masses over the Gulf of Mexico, J. Aerosol Sci., 19(5), 539–551, doi:10.1016/0021-8502(88)90206-6, 1988.

Schnell, R. C.: Ice Nuclei in Seawater, Fog Water and Marine Air off the Coast of Nova Scotia: Summer 1975, J. Atmos. Sci., 34(8), 1299–1305, doi:10.1175/1520-0469(1977)034<1299:INISFW>2.0.CO;2, 1977.
30 Schnell, R. C.: Airborne ice nucleus measurements around the Hawaiian Islands, J. Geophys. Res., 87(C11), 8886–8890, doi:10.1029/JC087iC11p08886, 1982.

Schnell, R. C. and Vali, G.: Freezing nuclei in marine waters, Tellus, 27(3), 321–323, doi:10.1111/j.2153-3490.1975.tb01682.x, 1975.

Schnell, R. C. and Vali, G.: Biogenic Ice Nuclei: Part I. Terrestrial and Marine Sources, J. Atmos. Sci., 33(8), 1554–1564, doi:10.1175/1520-0469(1976)033<1554:BINPIT>2.0.CO;2, 1976.

Spracklen, D. V. and Heald, C. L.: The contribution of fungal spores and bacteria to regional and global aerosol number and ice nucleation immersion freezing rates, Atmos. Chem. Phys., 14(17), 9051–9059, doi:10.5194/acp-14-9051-2014, 2014.

5   Stein, A. F., Draxler, R. R., Rolph, G. D., Stunder, B. J. B., Cohen, M. D. and Ngan, F.: NOAA's HYSPLIT Atmospheric Transport and Dispersion Modeling System, Bull. Am. Meteorol. Soc., 96(12), 2059–2077, doi:10.1175/BAMS-D-14-00110.1, 2015.

Tobo, Y., Prenni, A. J., DeMott, P. J., Huffman, J. A., McCluskey, C. S., Tian, G., Pöhlker, C., Pöschl, U. and Kreidenweis, S. M.: Biological aerosol particles as a key determinant of ice nuclei populations in a forest ecosystem, J. Geophys. Res.

10 Atmos., 118(17), 10,100-10,110, doi:10.1002/jgrd.50801, 2013.

Tobo, Y., DeMott, P. J., Hill, T. C. J., Prenni, A. J., Swoboda-Colberg, N. G., Franc, G. D. and Kreidenweis, S. M.: Organic matter matters for ice nuclei of agricultural soil origin, Atmos. Chem. Phys., 14(16), 8521–8531, doi:10.5194/acp-14-8521-2014, 2014.

Vali, G.: Quantitative Evaluation of Experimental Results an the Heterogeneous Freezing Nucleation of Supercooled

15 Liquids, J. Atmos. Sci., 28(3), 402–409, doi:10.1175/1520-0469(1971)028<0402:QEOERA>2.0.CO;2, 1971.

Vali, G., DeMott, P. J., Möhler, O. and Whale, T. F.: Technical Note: A proposal for ice nucleation terminology, Atmos. Chem. Phys., 15(18), 10263–10270, doi:10.5194/acp-15-10263-2015, 2015.

Vergara-Temprado, J., Murray, B. J., Wilson, T. W., O'Sullivan, D., Browse, J., Pringle, K. J., Ardon-Dryer, K., Bertram, A. K., Burrows, S. M., Ceburnis, D., DeMott, P. J., Mason, R. H., O'Dowd, C. D., Rinaldi, M. and

20 Carslaw, K. S.: Contribution of feldspar and marine organic aerosols to global ice nucleating particle concentrations, Atmos. Chem. Phys., 17(5), 3637–3658, doi:10.5194/acp-17-3637-2017, 2017.

Wang, X., Sultana, C. M., Trueblood, J., Hill, T. C. J., Malfatti, F., Lee, C., Laskina, O., Moore, K. A., Beall, C. M., McCluskey, C. S., Cornwell, G. C., Zhou, Y., Cox, J. L., Pendergraft, M. A., Santander, M. V., Bertram, T. H., Cappa, C. D., Azam, F., DeMott, P. J., Grassian, V. H. and Prather, K. A.: Microbial Control of Sea Spray Aerosol Composition: A Tale of

25 Two Blooms, ACS Cent. Sci., 1(3), 124–131, doi:10.1021/acscentsci.5b00148, 2015.

Westbrook, C. D. and Illingworth, A. J.: Evidence that ice forms primarily in supercooled liquid clouds at temperatures > −27°C, Geophys. Res. Lett., 38(14), L14808, doi:10.1029/2011GL048021, 2011.

Wex, H., Demott, P. J., Tobo, Y., Hartmann, S., Rösch, M., Clauss, T., Tomsche, L., Niedermeier, D. and Stratmann, F.: Kaolinite particles as ice nuclei: Learning from the use of different kaolinite samples and different coatings, Atmos. Chem.

30 Phys., 14(11), 5529–5546, doi:10.5194/acp-14-5529-2014, 2014.

Wheeler, M. J., Mason, R. H., Steunenberg, K., Wagstaff, M., Chou, C. and Bertram, A. K.: Immersion Freezing of Supermicron Mineral Dust Particles: Freezing Results, Testing Different Schemes for Describing Ice Nucleation, and Ice Nucleation Active Site Densities, J. Phys. Chem. A, 119(19), 4358–4372, doi:10.1021/jp507875q, 2015.

Wilson, T. W., Ladino, L. A., Alpert, P. A., Breckels, M. N., Brooks, I. M., Browse, J., Burrows, S. M., Carslaw, K. S., Huffman, J. A., Judd, C., Kilthau, W. P., Mason, R. H., McFiggans, G., Miller, L. A., Nájera, J. J., Polishchuk, E., Rae, S., Schiller, C. L., Si, M., Temprado, J. V., Whale, T. F., Wong, J. P. S., Wurl, O., Yakobi-Hancock, J. D., Abbatt, J. P. D., Aller, J. Y., Bertram, A. K., Knopf, D. A. and Murray, B. J.: A marine biogenic source of atmospheric ice-nucleating

5   particles, Nature, 525(7568), 234–238, doi:10.1038/nature14986, 2015.

Worringen, A., Kandler, K., Benker, N., Dirsch, T., Mertes, S., Schenk, L., Kästner, U., Frank, F., Nillius, B., Bundke, U., Rose, D., Curtius, J., Kupiszewski, P., Weingartner, E., Vochezer, P., Schneider, J., Schmidt, S., Weinbruch, S. and Ebert, M.: Single-particle characterization of ice-nucleating particles and ice particle residuals sampled by three different techniques, Atmos. Chem. Phys., 15(8), 4161–4178, doi:10.5194/acp-15-4161-2015, 2015.

10   Yakobi-Hancock, J. D., Ladino, L. A., Bertram, A. K., Huffman, J. A., Jones, K., Leaitch, W. R., Mason, R. H., Schiller, C. L., Toom-Sauntry, D., Wong, J. P. S. and Abbatt, J. P. D.: CCN activity of size-selected aerosol at a Pacific coastal location, Atmos. Chem. Phys., 14(22), 12307–12317, doi:10.5194/acp-14-12307-2014, 2014.

Yun, Y. and Penner, J. E.: An evaluation of the potential radiative forcing and climatic impact of marine organic aerosols as heterogeneous ice nuclei, Geophys. Res. Lett., 40(15), 4121–4126, doi:10.1002/grl.50794, 2013.

Table 1. The three sampling locations used in this study and conditions during sampling including average ambient temperature (T) and relative humidity (RH).

Location	Coordinates	Sampling period	Average sampling time (h)	Average ambient T (ºC)	Average ambient RH (%)	Average wind speed (m/s)
Amphitrite Point, BC, Canada	48.92º N, 125.54º W	8-27 August 2013	7.8	14	97	4.0
Labrador Sea, NL, Canada	54.59º N, 55.61º W	11 July 2014	6.2	10.9	70	5.4
Lancaster Sound, NU, Canada	74.26º N, 91.46º W	20 July 2014	5.3	2.8	95	4.6

Figure 1. Map showing the three sampling locations: Amphitrite Point (red dot), Labrador Sea (green dot), and Lancaster Sound (yellow dot). Inserts show the images of the sampling platform used at each location.
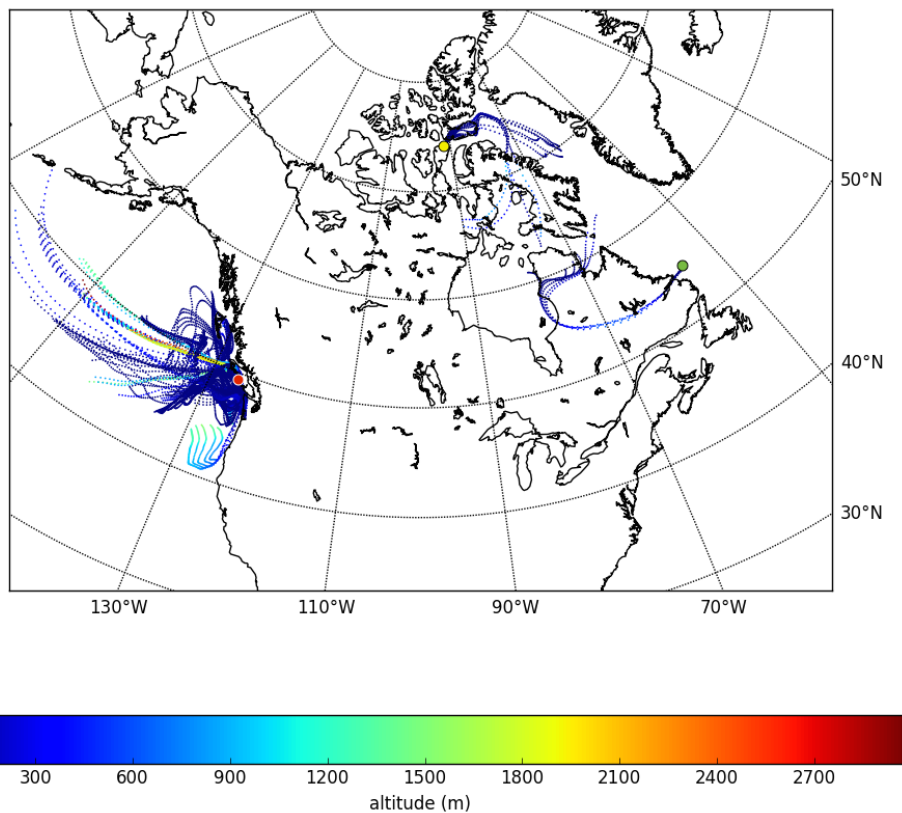
Figure 2. The 3-day HYSPLIT back trajectories for Amphitrite Point (red dot), Labrador Sea (green dot) and Lancaster Sound (yellow dot). The back trajectories were calculated for every hour during sampling period. The altitude is indicated with the colour scale. Global Data Assimilation System (GDAS) meteorological data at 1º x 1º spatial resolution was used as input to calculate the back trajectories using HYSPLIT.
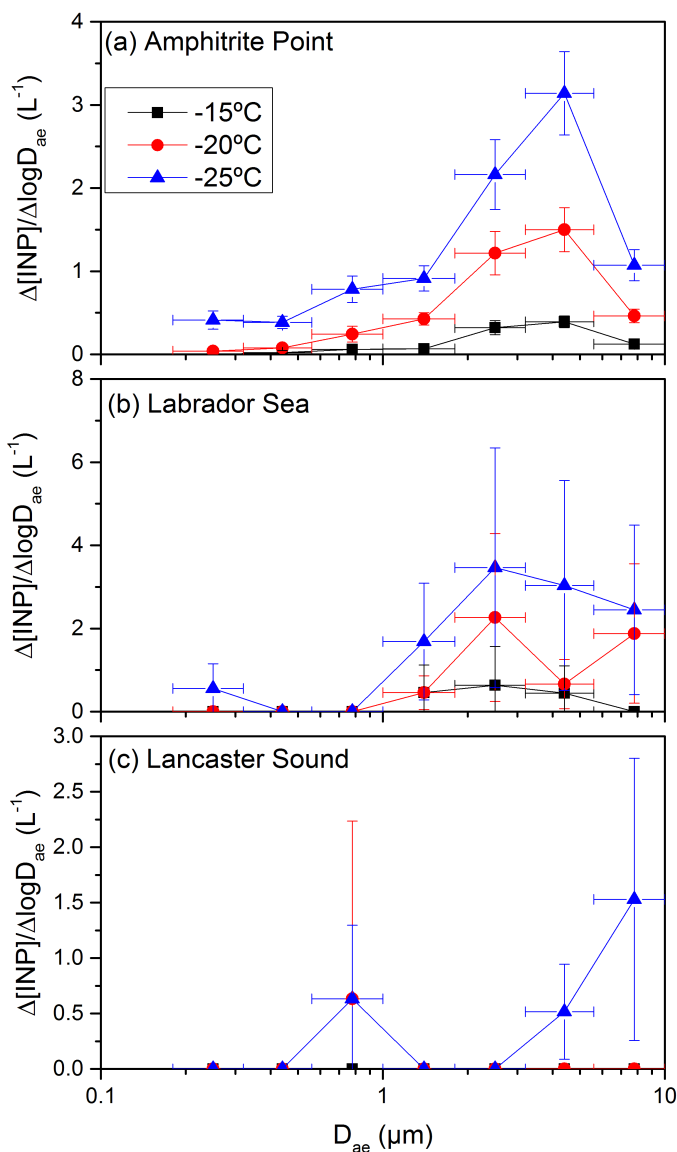
Figure 3. Average INP number concentrations at freezing temperatures of -15 °C, -20 °C, and -25 °C as a function of aerodynamic diameter (D_{ae}) for the three sites studied. The x-error bars represent the widths of the size bins from the MOUDI. For the Amphitrite Point samples, standard error of the mean was used to represent the uncertainty of INP concentrations during the month. At both Labrador Sea and Lancaster Sound, only one MOUDI sample was collected, and we assume the monthly INP concentrations has the same normal distribution as the Amphitrite Point samples. Hence for the y error bars at these locations, we assume the relative standard deviation for supermicron and submicron particles were the same as the relative standard deviation for supermicron and submicron particles observed in the Amphitrite Point data.
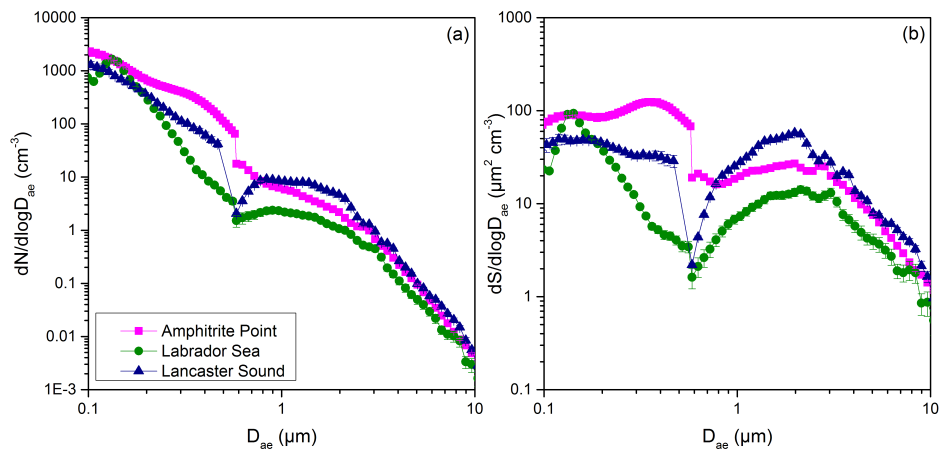
Figure 4. Concentrations of (a) aerosol number, N, and (b) surface area, S, as a function of aerodynamic diameter, D_{ae}. The y-error bars represent the standard error of the mean for each size bin. In many cases, the error bars are smaller than the size of the symbols. For cases where a gap existed between the two data sets, a straight line was used to extrapolate the data.
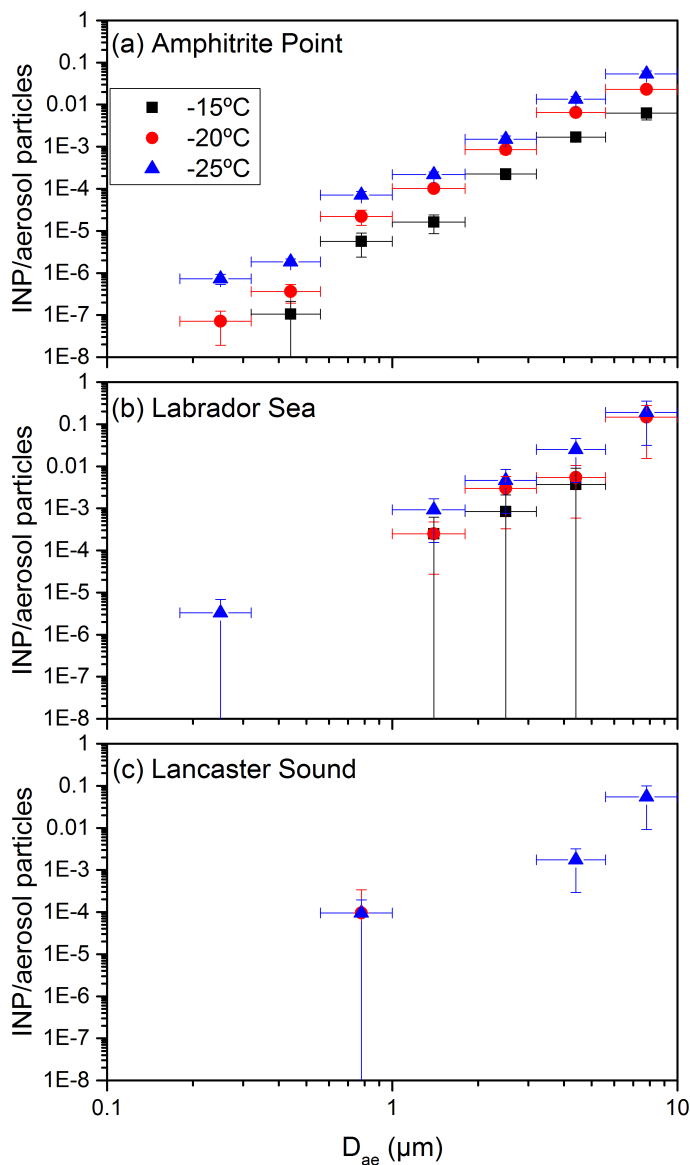
Figure 5. The fraction of aerosol particles acting as an INP as a function of aerodynamic diameter (D_{ae}) at -15 ºC, -20 ºC, and -25 ºC, respectively. The x-error bars represent the widths of the size bins, and the y-error bars are the propagated uncertainties from INP concentrations as a function of size (Fig. 3) and aerosol number concentrations as a function of size (Fig. S3a). In some cases, the y-error bars are smaller than the size of the symbols.
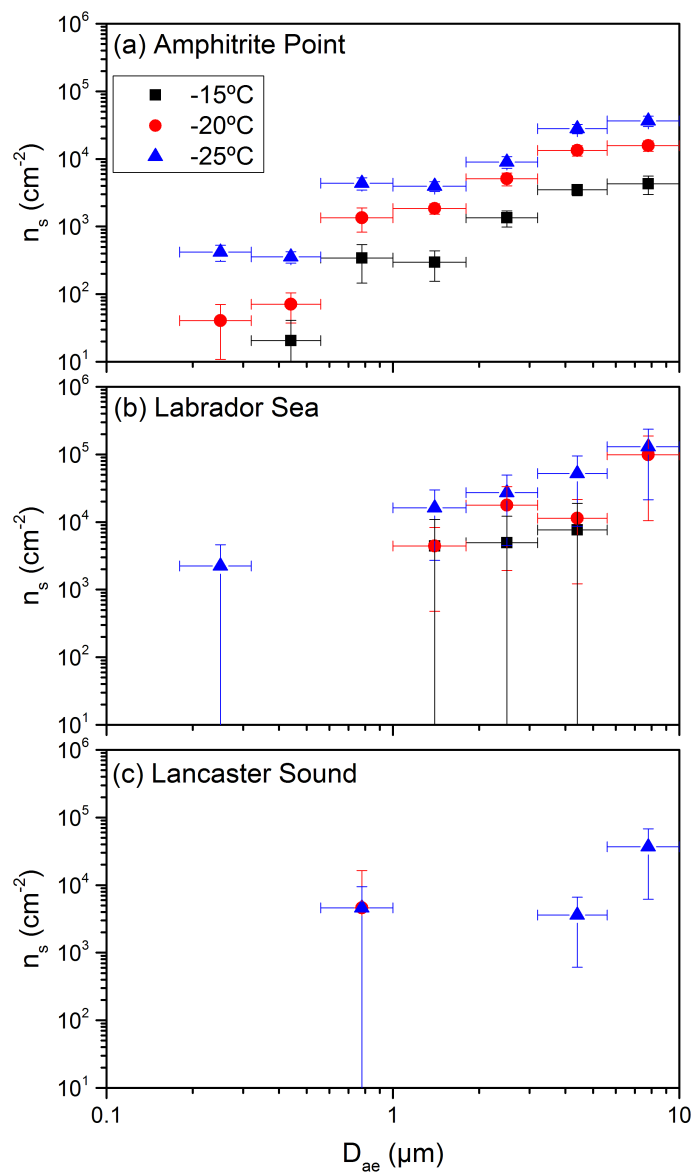
Figure 6. Surface active site density, n_s, as a function of aerodynamic diameter (D_{ae}) at -15 ºC, -20 ºC, and -25 ºC, respectively. The x-errors represent the widths of the size bins, and the y-errors are the propagated uncertainties from INP concentrations as a function of size (Fig. 3) and aerosol surface area concentrations as a function of size (Fig. S3b). In some cases, the y-error bars are smaller than the size of the symbols.
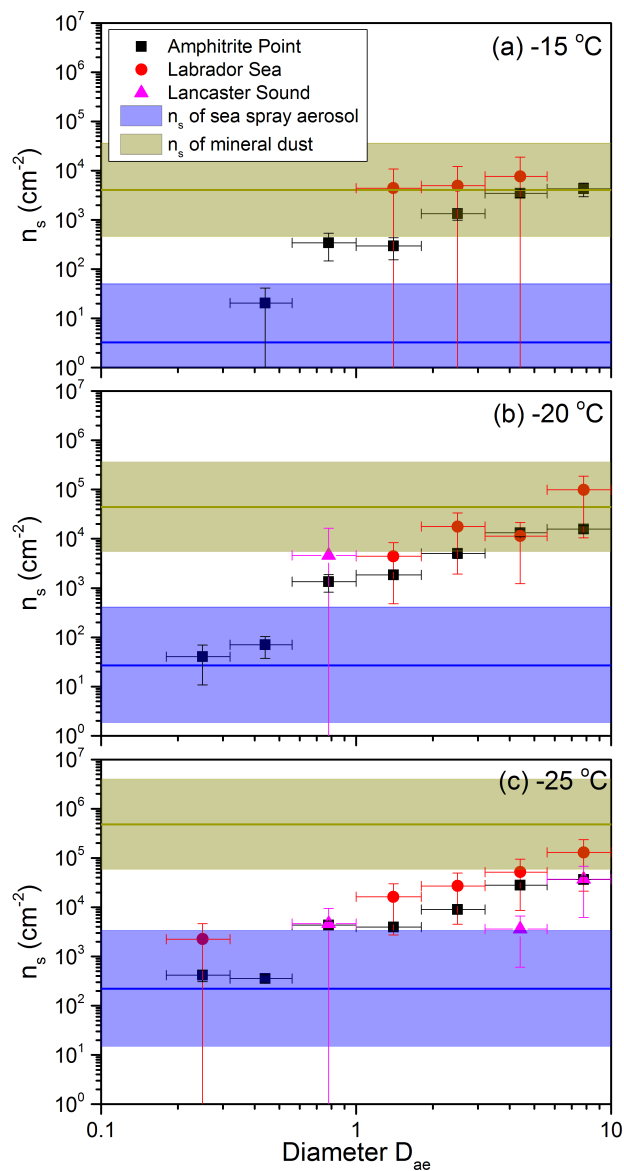
Figure 7. Comparison of measured n_s values with previously reported n_s values of sea spray aerosol and mineral dust at -15 °C, -20 °C, and -25 °C, respectively. The n_s values of sea spray aerosol were taken from DeMott et al. (2016), and the n_s values of mineral dust were taken from Niemand et al. (2012). The horizontal lines represent the calculated n_s values from linear regression, and the coloured bands represent the 95% prediction bands (see Fig. S4-S5 in the Supplement). Blue represents sea spray aerosol, and light green represents mineral dust.
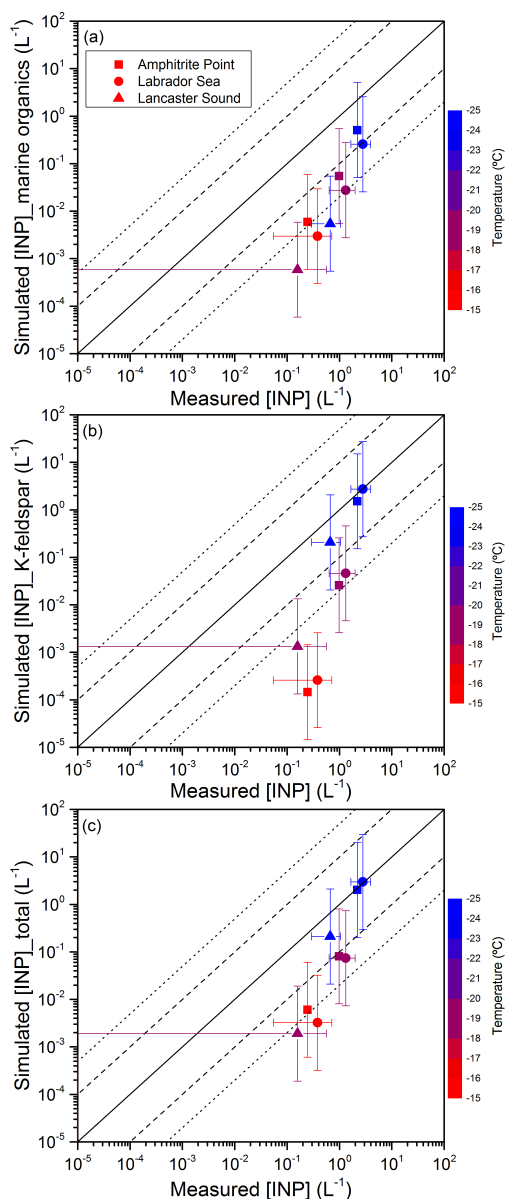
Figure 8. Comparison of measured INP concentrations and (a) simulated INP concentrations from marine organics, (b) simulated INP concentrations from K-feldspar, and (c) simulated INP concentrations from both. The solid lines represent 1:1 ratio, the

dashed and dotted lines represent one order and 1.5 orders of magnitude difference, respectively. The temperature is shown using a color map. The simulated INP concentrations for Amphitrite Point, Labrador Sea, and Lancaster Sound correspond to mean concentrations for the months of August, July, and July, respectively. The uncertainties in the simulated concentrations are estimated to be around one order of magnitude based on the parameterization and model uncertainty (Harrison et al., 2016; Wilson et al., 2015).